Analysis and compensation of thermal lens effects in Tm:YAP lasers

Baoquan Yao (姚宝权)*, Yi Tian (田 义), Wei Wang (王 维), Gang Li (李 纲), and Yuezhu Wang (王月珠)

National Key Laboratory of Tunable Laser Technology, Harbin Institute of Technology, Harbin 150080, China

**E-mail: yaobq08@126.com*

Received April 21, 2010

The thermal lens effects in Tm:YAP laser are analyzed by solving the Poisson equation with finite difference method. The thermal focal lengths measured are in the range of 40 − 90 mm at the pump power of 16 − 34 W, consistent with the simulation results. The temperature contribution coefficient (the linear coefficient between the maximum temperature in the laser crystal and the pump power) of 1.19 K/W is also obtained. The convex lens and plano-concave mirror thermal lens compensation methods are proposed and applied to a high power pumped Tm:YAP laser.

OCIS codes: 140.3410, 140.3580, 140.6810.

doi: 10.3788/COL20100810.0996.

Solid-state lasers in the eye-safe range of 2 μm[1] are important owing to the potential applications in atmospheric sounding[2], wind lidar[3], medicine[4−6], and so on. Tm^{3+} doped $YAlO_3$ crystal has advantages in high-power laser operation due to its high mechanical strength and large heat conductivity (0.11 W/(cm·K))[7], which allows high-power operation with reduced risk of fracture. The main problem that limits the power scaling of Tm:YAP lasers is the generation of heat inside the crystal. The generated heat causes steep temperature gradients inside the gain medium, which in turn induce instability of the resonator, and hence affect the laser output. Thermal lens effects in other Tm^{3+} doped or Tm^{3+}, Ho^{3+} co-doped crystals have been discussed in Refs. [8−10]. However, the compensation of the thermal lens effects has not been discussed in those papers. Therefore, it is significant to discuss the thermal lens effects in Tm:YAP crystal, and propose methods to compensate the thermal lens effects.

In this letter, the temperature distribution in the crystal is numerically simulated by solving the Poisson equation with finite difference method. The thermal focal length is also calculated by considering the assumption of thermally induced spherical convex lens. These results are compared with the experimental measurement data. Two sorts of resonators are designed to compensate the thermal lens effects.

In the situation of heat balance, the temperature distribution in the crystal can be described by three-dimensional (3D) Poissonal equation as[11]

$$K_x \frac{\partial^2 T(x,y,z)}{\partial x^2} + K_y \frac{\partial^2 T(x,y,z)}{\partial y^2} + K_z \frac{\partial^2 T(x,y,z)}{\partial z^2} + q(x,y,z) = 0, \tag{1}$$

where x and y are the transverse coordinates, z is the longitudinal coordinate with the value of $z = 0$ at the pump end of crystal; K_x, K_y, K_z are respectively the heat conductivity coefficients of the three axis; T is the temperature; $q(x,y,z)$ is the thermal density along the resonator axis in the crystal which can be written as

$$q(x,y,z) = \frac{2Q\alpha}{\pi\omega_{\rm p}^2(z)} \left(1-{\rm e}^{-\alpha L}\right) {\rm e}^{-2\left[\left(x-\frac{a}{2}\right)^2+\left(x-\frac{b}{2}\right)^2\right]/\omega_{\rm p}^2(z)-\alpha z} \tag{2}$$

with

$$\omega_{\rm p}(z) = \omega_{\rm p0} + \frac{2\lambda\pi \times M^2}{\omega_{\rm p0}} |z - z_0|, \tag{3}$$

where Q is the total heat load in the crystal, α is the absorption coefficient, $\omega_{\rm p0}$ is the waist radius of the pump beam, L is the length of the crystal, a and b are the transverse size of the crystal, λ is the wavelength, M^2 is the pump beam quality, and z_0 is the distance between the focal plane of pump beam and the pumped facet of laser medium. After knowing the temperature distribution, we can calculate the optical path difference (OPD) for one pass through the crystal. The OPD can be written as[12]

$$\mathrm{OPD}(x,y) = 2\left[\int_0^L \frac{\partial n}{\partial t} T(x,y,x){\rm d}z + n_0 \Delta u(x,y) + \sum_{i,j=1}^{3} \int_0^L \frac{\partial n}{\partial \varepsilon_{i,j}} \varepsilon_{i,j}(x,y,z){\rm d}z\right], \tag{4}$$

where the first term in the brackets is caused by the thermal dispersion ${\rm d}n/{\rm d}T$, the second term results from the change induced by z-axis expansion ${\rm d}u/{\rm d}z$, and the third term stands for the strain-induced birefringence with the strain tensor ε_{ij}. In the pumped region, it is common to consider the laser crystal to be a thermally induced spherical convex lens. So, the focal length of the thermal lens can be derived from Eq. (4) as

$$f(x,y) = \frac{x^2+y^2}{2[\mathrm{OPD}_0 - \mathrm{OPD}(x,y)]}, \tag{5}$$

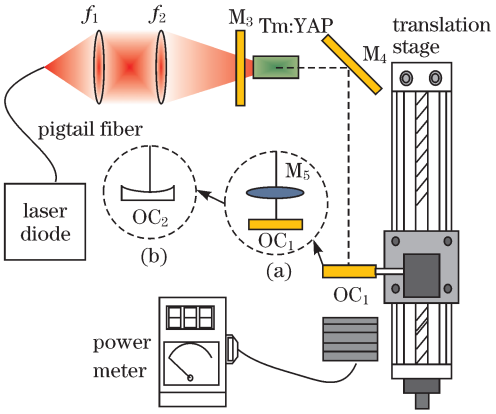

Fig. 1. Thermal focal length measurement device. f_1, f_2: pump beam focusing lenses; M_3: HR at 1.94 μm, AR at 792 nm; M_4: 45° HR at 1.94 μm, AR at 792 nm; M_5: compensation convex lens; OC_1: plane output coupler; OC_2: plano-concave mirror, $T = 10\%$ at 1.94 μm.

where OPD_0 is the OPD in the center.

Figure 1 shows the schematic layout of the experimental setup used for measuring the thermal focal length. The pumping light (DILAS Diodenlaser GmbH, coupled by LIMO fiber, numerical aperture (NA) 0.22, diameter = 0.2 mm) is focused on the center of the crystal. f_1(f = 51 mm) and f_2 (f = 100 mm) are collimating and focusing lenses. The focused pump beam in the laser medium has a diameter of about 392 μm. A c-cut Tm:YAP crystal which has a size of $a \times b \times c = 3\times3\times8$ (mm) with the refractive index of 1.94 was used in simulation and experiment[13]. The crystal was wrapped with indium foil and fitted into a copper heat sink which was cooled by thermoelectric cooler (TEC) at the temperature of T_0 = 288 K. The thermal conductivity of copper is large enough to be considered as an invariable boundary condition. The Tm:YAP sample has a Tm^{3+}-doping concentration of 4 at.-%. Both sides of the sample are anti-refection (AR) coated at ~2 μm to decrease the optical loss. The input mirror (M_3) was high-reflection (HR) coated in a broad band at 1.94 μm and AR coated at 792 nm. M_4 is a 45° reflector (HR at 1.94 μm). The output coupler (OC) is a plane mirror with a transmittance of 10%. The OC is fixed to a translation stage, which is used for adjusting the cavity length. Due to the thermal lens effects, the laser output power would fall down to zero as the pump rise up when the thermal focal length makes the resonator unstable. The corresponding pump power is recorded at different cavity lengths. According to $ABCD$ matrix, the thermal focal length can be calculated.

The parameters used for solving the equation by finite difference method are shown in Table 1. Figure 2 shows the temperature distribution in $x-z$ section at the pump power of 34 W (y = 0). The highest temperature in the crystal is 328 K at the center of the pump end face, in contrast to 288 K boundary value. The temperature decreases along the z-axis. The straight line in Fig. 3 shows that the maximum temperature in the laser crystal is approximately linear with respect to the pump power P_p. The mathematical relationship can be expressed as $T_{max} = \eta_{max} P_p + T_0$. The linear coefficient η_{max} is defined as temperature contribution coefficient of 1.19 K/W

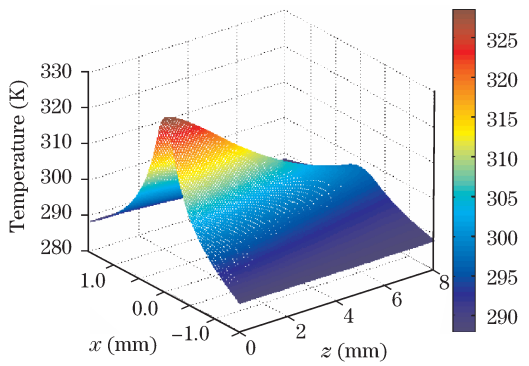

Fig. 2. Temperature distribution in x-z section (y = 0) at the pump power of 34 W.

Table 1. Parameters Used in Numerical Simulation

Parameter	Value	Parameter	Value
du/dz[14]	$5.1\times10^{-6}K^{-1}$	z_0	1 mm
Heat Fraction η[15]	0.22	M^2	87
α	1.5 cm^{-1}	ω_p	196 μm
dn/dT	$14.6\times10^{-6}K^{-1}$	λ	792 nm
K_z	0.11 W/(cm·K)	Poisson Ratio	0.3

obtained from the above equation.

Figure 3 shows the focal length of the thermal lens. Compared with the experimental results (squares), our numerical simulation (solid curve) shows good accordance. In Fig. 3, the dashed line is acquired by an analytical model[16]:

$$f_T = \frac{\pi K_c \omega_p^2}{P_{ph}\,(dn/dt)} \left[\frac{1}{1-e^{-\alpha L}}\right], \qquad (6)$$

where f_T is the focal legth.

The analytical curve is lower than the experimental results. In the explanation of Ref. [11], the error is attributed to the influence from the end face curvature (thermal expansion) which is neglected in the formula. By considering Eqs. (4) and (5), it is quite obvious that OPD_0 will increase faster than OPD(x,y) ($x^2+y^2 \neq 0$) for the temperature in the center higher than the boundary, when the end face curvature is considered. Therefore, the focal length f_T will be lower than actual values correspondingly. For not considering the thermal expansion in Eq. (6), the theoretical data should be larger than the experimental data. However, these results disagree with the fact. Actually, one reason is that the pump beam radius is considered as a constant in the derivation of Ref. [16]. The change of beam radius along the z-axis in the crystal cannot be neglected since the pump beam has a M^2 factor of 87. The heat distribution along the z-axis is uneven and dispersive, which means that the thermal effect of the gain medium is weakened. Therefore, the results of the analytical model are lower than the numerical simulation results and experimental data.

After the focal length of thermal lens is measured, the resonators to compensate the thermal lens effects are designed. For keeping the cavity stable, a convex lens is inserted inside the resonator. The lens has a focus length (f) of 100 mm. The scheme of the device is shown in

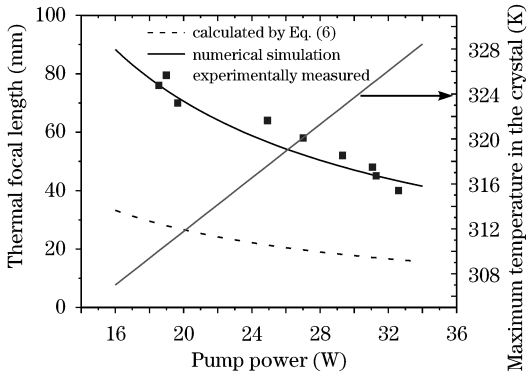

Fig. 3. Thermal focal length and the maximum temperature of the crystal versus pump power.

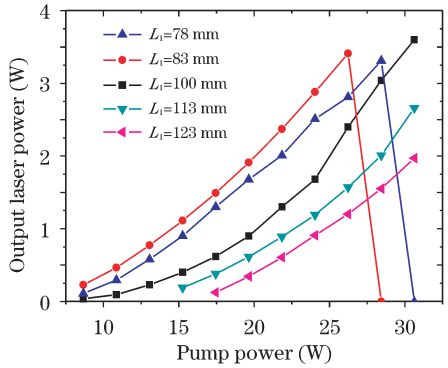

Fig. 4. Output laser power versus pump power with different L_1 (f = 100 mm).

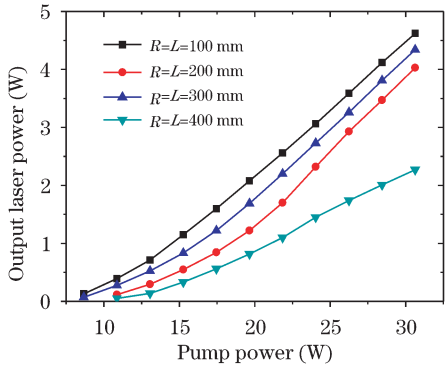

Fig. 5. Output laser power versus pump power with different OCs ($R = L_2$ = 100, 200, 300, 400 mm).

inset (a) of Fig. 1. L_1 is the distance between the center (z-direction) of the laser crystal and the convex lens. The laser output power versus the pump power is measured by Coherent PM30 power meter with different L_1 values, as shown in Fig. 4. If $L_1 < 100$ mm, the output power falls to zero when the pump power $P >$ 25 W, which means that the thermal lens makes the resonator unstable. However, the output power does not fall when P is larger than 25 W at $L_1 \geq 100$ mm. With L_1 increasing from 100 to 123 mm, the slope efficiency and the maximum output power decrease obviously. The maximum output power and slope efficiency are obtained when the lens is changed to the right position (L_1 = 100 mm). As it turns out, the lens focuses on the middle of the crystal. The result shows that convex lens focusing on the center of the crystal has the best effect on compensating thermal focal length.

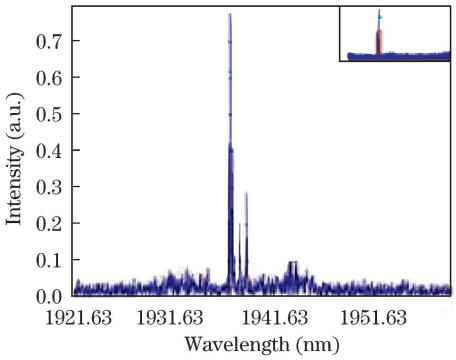

Fig. 6. Output laser spectrum.

Another kind of compensation device is achieved with a plano-concave mirror as an output coupler (OC_2), as shown in inset (b) of Fig. 1. Here, L_2 indicates the distance between the middle of laser crystal and OC_2. Four plano-concave mirrors with different radii (100, 200, 300, and 400 mm) but the same transmittance of 10% at 1.94 μm are selected in this experiment. Because plano-concave mirror has the similar $ABCD$ matrix form [1, 0; $-2/R$, 1] as convex lens [1, 0; $-1/f$, 1], L_2 is equal to the plano-concave mirror's radius (R) for every mirrors used in this cavity. Figure 5 shows the output laser power as a function of the pump power. No laser power break phenomenon is observed until the pump power reaches the largest, which indicates that the resonator keeps stable, and the plano-concave mirror can also compensate the thermal focal length. The maximum output laser power at $R = L_2$ = 100 mm is 1.02 W higher than the convex lens thermal lens compensation method ($f = L_1$ = 100 mm) (3.6 W). That is mainly due to the lower cavity loss while no extra lens is inserted in the resonator. The output laser spectrum is measured by EXFO WA1500 wavelength meter, as shown in Fig. 6.

In conclusion, the thermal lens effects in Tm:YAP laser are analyzed by numerical and analytical methods. We find that the maximum temperature in the laser crystal is approximately linear with respect to the pump power, and the temperature contribution coefficient is 1.19 K/W. The experimental results of thermal focal length agree with the numerical model well. However, the results of the analytical model are lower than the experimental data because of neglecting the pump beam distribution along the axis of the crystal. Two thermal lens compensation methods are proposed. One method is that the focal length of convex lens is set to the middle of the laser crystal, and the other is that the radius of the plano-concave mirror is also set to the middle of the crystal. The effectiveness of these methods is experimentally proved.

References

1. T. Yokozawa, and H. Hara, Appl. Opt. **35,** 1424 (1996).
2. G. J. Koch, B. W. Barnes, M. Petros, J. Y. Beyon, F. Amzajerdian, J. Yu, R. E. Davis, S. Ismail, S. Vay, M. J. Kavaya, and U. N. Singh, Appl. Opt. **43,** 5092 (2004).

3. V. Wulfmeyer, M. Randall, A. Brewer, and R. M. Hardesty, Opt. Lett. **25,** 1228 (2000).
4. T. Bilici, Ö. Tabakoğlu, H. Kalaycloğlu, A. Kurt, A. Sennaroğlu, and M. Gülsoy, in *CLEO/Europe and EQEC 2009 Conference Digest* CL_P11 (2009).
5. H. Jelínková, P. Koranda, J. Šulc, M. Němec, P. Černý, and J. Pašta, Proc. SPIE **6871,** 68712N (2008).
6. C. Wu, Y. Ju, Y. Li, Z. Wang, and Y. Wang, Chin. Opt. Lett. **6,** 594 (2008).
7. Y. Li, B. Yao, Y. Wang, Y. Ju, G. Zhao, Y. Zong, and J. Xu, Chin. Opt. Lett. **5,** 286 (2007).
8. E. H. Bernhardi, A. Forbes, C. Bolig, and M. J. D. Esser, **16,** 11115 (2008).
9. W.-J. He, B.-Q. Yao, Y.-Z. Wang, and Y.-L. Ju, Acta Phys. Sin. (in Chinese) **56,** 3240 (2007).
10. X.-L. Zhang, Y.-Z. Wang, and H.-F. Shi, Acta Phys. Sin. (in Chinese) **55,** 1787 (2006).
11. T. Li, S. Zhao, Z. Zhuo, and Y. Wang, Opt. Commun. **282,** 940 (2009).
12. C. Pfistner, R. Weber, H. P. Weber, S. Merazzi, and R. Gruber, IEEE J. Quantum Electron. **30,** 1605 (1994).
13. B. Yao, X. Duan, Y. Li, L. Zheng, Y. Wang, G. Zhao, and J. Xu, Chin. Opt. Lett. **6,** 520 (2008).
14. Y. Lu, Y. Dai, Y. Yang, J. Wang, A. Dong, and B. Sun, J. Alloy. Compd. **453,** 482 (2008).
15. P. Černý and D. Burns, IEEE J. Sel. Top. Quantum Electron. **11,** 674 (2006).
16. M. E. Innocenzi, H. T. Yura, C. L. Fincher, and R. A. Fields, Appl. Phys. Lett. **56,** 1631 (1990).